ARTICLE

DFT investigation on Lewis base-catalyzed Lewis acid-mediated reactions: Hypervalent silicon species as chiral organocatalysts in (direct) aldol reactions

Received 00th January 20xx,
Accepted 00th January 20xx

DOI: 10.1039/x0xx00000x

Sergio Rossi,*[a] Maurizio Benaglia [a] and Laura Maria Raimondi [a]

The stereoselective organocatalytic addition of silyl enol ethers to aromatic aldehydes catalyzed by bisphosphoroamides and the direct aldol reaction between ketones and aromatic aldehydes promoted by phosphinoxides in the presence of tetrachlorosilane were investigated by DFT approach. The formation of different chiral cationic hypervalent silicon species was investigated by calculations. Investigation on Lewis base catalyzed Lewis acid mediated cross aldol reactions were also performed.

Introduction

Hypervalent silicon compounds have generated great interest since their first discovery performed by Gay-Lussac in the nineteenth century.[1] Nowadays, the ability of silicon to form more bonds than the four predicted by the rules of primary valence is well documented and this extra-coordination has been exploited in the development of many organocatalyzed and enantioselective reactions involving different silicon-based Lewis acids (LA).[2-7] The ability of silicon to break the "Lewis–Langmuir octet rule" is related to the fact that when a Lewis acidic silicon species interacts with a donor molecule (a Lewis base, LB), it leads to the formation of a new highly reactive adduct, endowed with enhanced electrophilic character.

Different theories have tried to explain this particular behaviour,[8-19] but the most accepted one involves a reorganization of the electronic density around the silicon atom, as predicted by the Gutmann' semiempirical analysis.[20] Following this statement, the coordination of a Lewis basic donor ligand causes an enhanced activity of a Lewis acidic silicon acceptor, in which the central atom of the Lewis acid becomes more electrophilic, causing a transfer of electron density on the peripheral ligands. This results in the ionization of one of the ligands from the Lewis acid, emphasizing the Lewis acidity of the central atom and generating a new species with improved activity. According to this mechanism, a poorly Lewis acidic silicon species could be activated upon binding of a Lewis base, thus generating a cationic species, a new stronger acid.[5, 7, 21] This activation mode is at the base of the class of reactions named "Lewis base-catalysed Lewis acid-mediated reactions", where a small amount of a Lewis base (generally phosphoramides and phosphinoxides) acts as a catalyst in the activation of $SiCl_4$, present in stoichiometric amount. Although many types of chiral phosphoramides and phosphinoxides have been used to promote different organocatalytic and stereoselective transformations, computational investigations aimed to the study of the mechanisms responsible of the stereochemical outcome of these reactions has never been explored in details. Usually, stereoselectivity has been explained with reasonable but empirical stereoselectivity models. In this paper we wish to report our DFT analysis on transition states involved in some diastereoselective (direct) aldol-type reactions.

Results and Discussion

In 2003 prof. Denmark reported the stereoselective addition of silyl enol ethers to aromatic aldehydes, one of the first examples of LB-catalyzed LA-mediated reaction developed for the formation of new carbon-carbon bonds.[22] In this transformation, silicon tetrachloride can be activated by a catalytic amount of the chiral bisphosphoramide (**1**) derived from chiral (*R*)-*N,N'*-dimethyl-binaphthyl diamine to form a highly reactive, chiral trichlorosilyl cation, which is the effective promoter of the aldol addition of a variety of unsubstituted silyl enol ethers to aromatic, olefinic, and heteroaromatic aldehydes in excellent yields (Scheme 1). The reaction proceeds rapidly at low temperatures, yielding the corresponding β-hydroxy ketones in high chemical and stereochemical efficiency. In a further detailed paper,[23] according to PM3 semiempirical calculations, it was postulated that the carbonyl oxygen of the aldehyde is bounded in a trans position to the phosphoramide P=O in according to the nature of the hypervalent bonds in the ligand field around silicon.[10] Furthermore, the presence of stabilizing π-π interaction between the aromatic ring of the aldehydes and one of the naphthyl rings of the catalyst in an edge-on fashion represent a potential controlling factor for the stereoselectivity (Figure 1, complex **ii**). According to this picture, the attack of the silyl enol ether occurs on the *Re* face of the aldehyde, since the skeleton of the catalyst acts as a shield to the *Si* face.

[a] Department of Chemistry, Università degli Studi di Milano, via Golgi 19, 20133 Milano, Italy. Corresponding author e-mail: sergio.rossi@unimi.it.

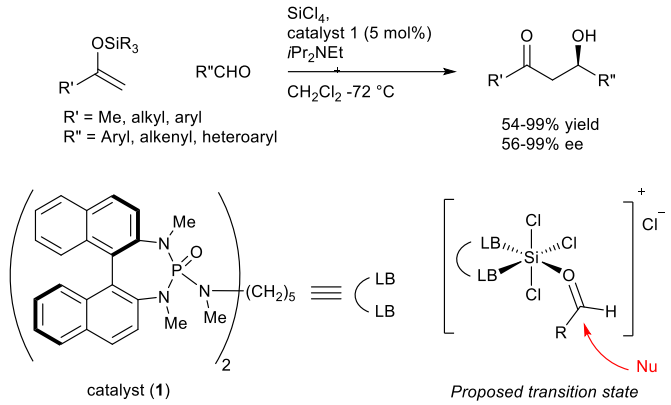

Scheme 1: Catalytic, enantioselective addition of silyl enol ethers to aldehydes promoted by bisphosphoramide **1**.

In order to support this hypothesis and to validate our computational approach, we initially investigated by DFT approach the coordination of benzaldehyde to the enantiopure hypervalent silicon species resulting from the coordination of catalyst **1** to $SiCl_4$. Initial geometries of complexes **i** and **ii** depicted in Figure 1 were obtained by Monte Carlo conformational analysis performed with Molecular Mechanics calculations using the OPLS_2005 force field[24] of the Macromodel package[25] in the Schrodinger suite.[26] Then, the two structures at lower energies were fully optimized by DFT approach using the B3LYP functional with 6-31G(d) basis set of Gaussian package.[27] As result, complex **ii** is favoured of 1.36 kcal mol^{-1} compared to complex **i**. This difference could be attributed essentially to the steric repulsion between the *N*-methyl group bounded to the binaphthyl ring and the benzaldehyde aromatic ring, which is higher in complex **i** than in complex **ii**. In addition, a non-covalent interaction (NCI) analysis, performed using the NCIPLOT software,[28-29] revealed that both complexes **i** and **ii** present a weak positive π–stacking interaction (showed as a green surface in Figure 1) between the phenyl ring of the aldehyde and the binaphthyl ring of the catalyst. Noteworthy, even if complex **i** has an extended interaction compared to complex **ii**, it is characterized by a face-to-face sandwich interaction which is known to be less favoured compared to the edge-to-face interaction of complex **ii**.[30-31]

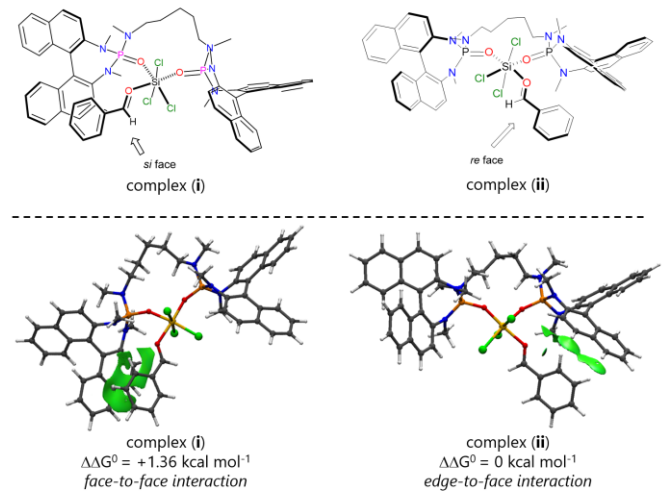

Figure 1: (op) structures related to benzaldehyde catalyst(**1**) coordination. (Bottom) NCIPLOT analysis of complex **i** (left) and complex **ii** (right) calculated at B3LYP/6-31G(d) level of theory.

This ground state catalyst-substrate complexes analysis does not offer a definitive answer for reaction selectivity, but it is in agreement with the experimental finding that using (*R,R*)-catalyst-(**1**), the *Re* face of the aldehyde is most favourably attacked by the silyl enol ether. On the basis of these results, both complex **i** and complex **ii** were used as starting point in the computational study of the catalytic, enantioselective addition of trimethyl silyl enol ether (**2**) to benzaldehyde, where, according to the original paper, β-hydroxy ketone (*R*)-**3** was obtained in 98% ee (Scheme 2).[22] A rationale for the observed enantioselectivity was already previously discussed, due to the different possible approaches of the silyl enol ether. [5,7,32] According to this analysis, the reaction proceeds through open transition structures, and two antiperiplanar (*ap*) and four synclinal (*sc*) transition structures can be hypothesized. Transition-state structures TS(**1**)-*Re-ap*$_1$, TS(**1**)-*Re-sc*$_1$, and TS(**1**)-*Re-sc*$_2$ produce (*R*) aldol adducts, whereas TS(**1**)-*Si-ap*$_2$, TS(**1**)-*Si-sc*$_3$ and TS(**1**)-*Si-sc*$_4$ afford (*S*) products. Due to the dipole–dipole interactions between the two carbon–oxygen bonds and to the steric repulsion between the phenyl and *i*-butyl groups, synclinal transition-states TS(**1**)-*Re-sc*$_1$ and TS(**1**)-*Si-sc*$_4$ are disfavoured.

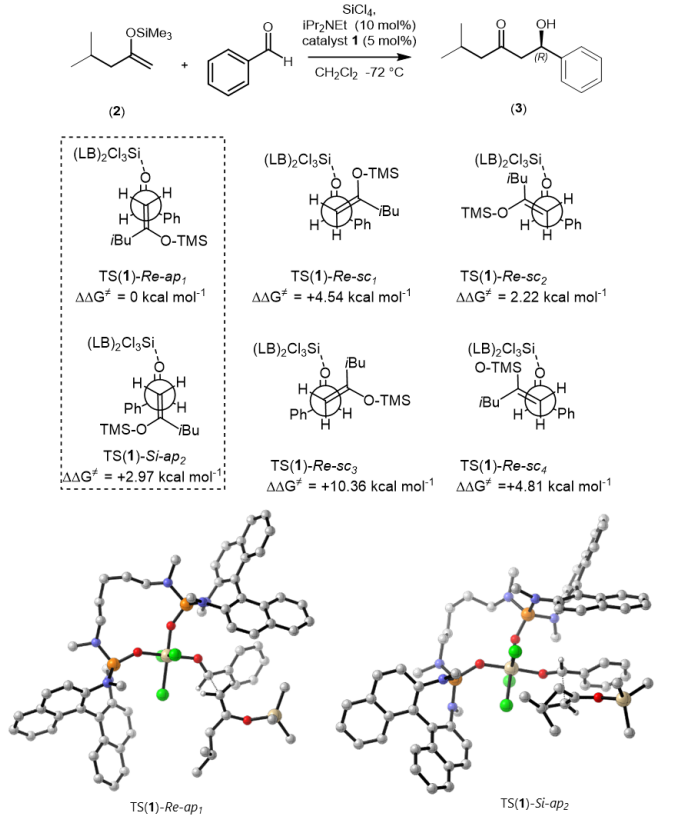

Scheme 2: B3LYP/6-31G(d) geometries related to the catalytic, enantioselective addition of trimethylsilylenol ether (**2**) to benzaldehyde.

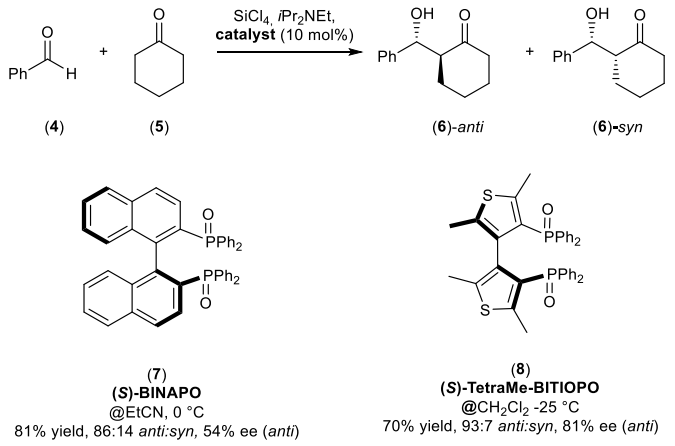

Scheme 3: Comparison between BINAPO and TetraMeBITIOPO activity in direct aldol reaction of cyclohexanone and benzaldehyde promoted in the presence of $SICl_4$.

In TS(**1**)-*Re*-*sc*$_2$ and TS(**1**)-*Si*-*sc*$_3$ there are disfavoured interactions between the *i*-butyl group and the carbonyl oxygen atom, therefore, only the two antiperiplanar transition states, responsible of the formation of both (*R*)- and (*S*)-**3** are accessible. All these transition states have been located at a B3LYP/6-31G(d) level of theory (both with one imaginary frequency); as expected TS(**1**)-*Re*-*ap*$_1$ responsible of the formation of the experimentally observed (*R*)-**3** enantiomer is the most favoured one compared to TS(**1**)-*Si*-*ap*$_2$ of 2.97 kcal mol^{-1}. Few years later, Nakajima demonstrated that also chiral bisphosphinoxides can act as efficient catalysts in the direct enantioselective aldol reactions; the generation of the silyl enol ethers from a carbonyl compound can be accomplished *in situ*, in the presence of tetrachlorosilane and a tertiary amine (Scheme 3).[33]

Also our group successfully extended the direct aldol condensation between carbonyls and aromatic aldehydes using the more electron-rich (*S*)-tetramethyl-bisthiophenphosphinoxide (*S*)-Tetra-Me-BITIOPO and its derivatives, obtaining the corresponding aldol products (**6**) often with higher yields and stereoselectivities compared to those observed using (*S*)-BINAPO.[34-40] In this transformation, as postulated by Nakajima and co-workers, the interaction of a ketone with the hypervalent silicon species generated by the phosphinoxide-$SiCl_4$ coordination leads to the *in situ* formation of a trichloro silylenol ether. As consequence, this enol ether results activated by the phosphinoxide to react with the aldehyde, allowing the formation of the desired β-hydroxy ketone. Even if the catalytic cycle of the direct aldol reaction was never been investigated experimentally in details, it must be noted that many computational analysis, conductivity studies[41] and Rapid Injection NMR investigations[42-44] were conducted to elucidate the nature of the interaction of hypervalent silicon Lewis species activated by the presence of mono- and bisphosphoramides. For analogy with those systems, it can be assumed that the interaction of $SiCl_4$ with phosphinoxides follows the same behaviour: upon coordination of the Lewis base with $SiCl_4$ and after an initial formation of a dimeric resting state, the ionization of a chloride ion occurs and the chiral, cationic pentavalent trichlorosilyl species **iii** is generated (Scheme 4).

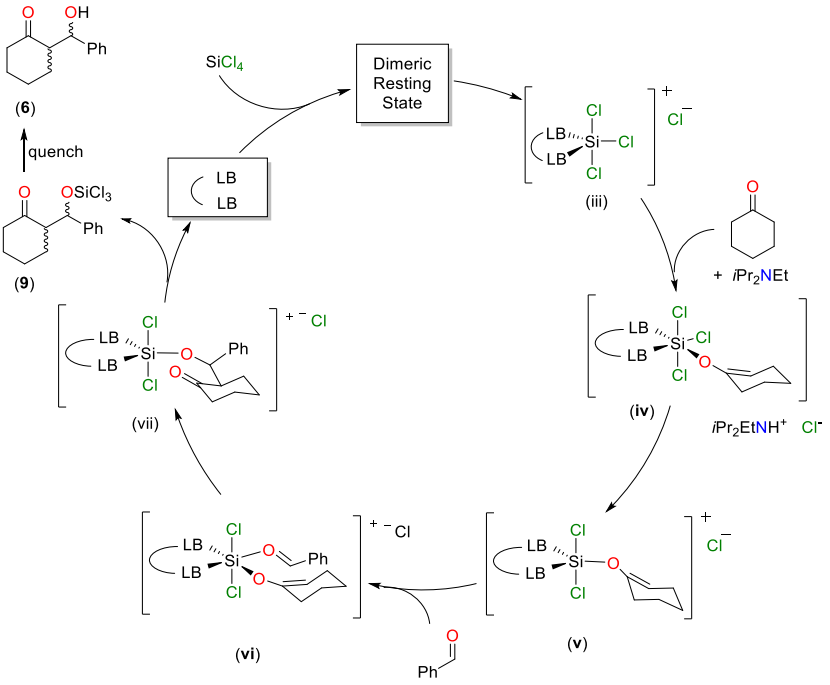

Scheme 4. Proposed mechanism of the enantioselective direct aldol reaction between ketones and aldehydes catalyzed by phosphinoxides. LB-LB = (*S*)-Tetra-Me-BITIOPO

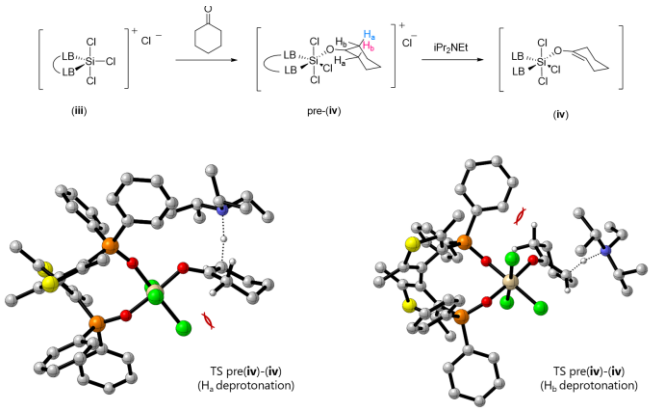

Scheme 5: TS-pre(**iv**) related to the deprotonation of cyclohexanone coordinated to the hypervalent specie **ii** calculated at B3LYP-D3/6-31G(d,p) level of theory.

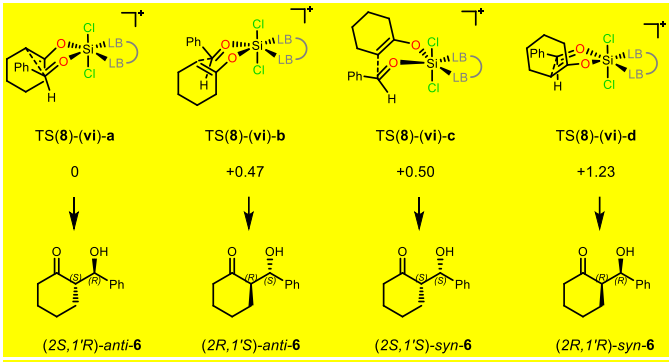

Scheme 6: $\Delta\Delta E^{\neq}$ of transitions states expressed in kcal mol^{-1} and calculated at B3LYP-D3/6-311+G(2df,2pd) // B3LYP-D3/6-31G(d,p) level of theory. LB-LB correspond to TetraMeBITIOPO **8**.

This new hypervalent species will then coordinate the ketone, which undergoes the attack of *i*Pr$_2$NEt base (present in the reaction media) to generate the neutral hypervalent chlorosilyl enol ether **iv**. Due to this transfer of electron density, an expulsion of a chlorine anion will occur, with the consequent formation of the cationic species **v** that in turn will coordinate a molecule of aldehyde generating species **vi.** The transition state responsible of the new bond formation of species **vii** is the key step of this transformation, is a cationic chair-like six membered ring species, which is responsible for the stereochemical outcome. From species **vii**, after the release of the Lewis Base (which re-enters in the catalytic cycle), the formation of β-trichlorosilyloxy ketone **9** occurs and a simple aqueous work-up will afford the expected β-hydroxy ketone **6**. Since the formation of hypervalent species **iii** was already experimentally demonstrated, we started our investigation with the analysis of specie **iv**. The computational analysis performed using the dispersion-inclusive density B3LYP-D3 functional with 6-31G(d,p) basis set revealed that the initial coordination of cyclohexanone to silicon hypervalent species is favoured in energy ($\Delta\Delta G^{\neq}$ values = -4.11 Kcal mol^{-1} for TS-(**iii**)pre(**iv**)); moreover, the approaching of the ketone occurs on the same plane containing the two P=O groups of the phosphine oxide, as predicted by the hypervalent bond theory. In the next step, the deprotonation by *i*Pr$_2$NEt takes place, generating species **iv.** Since catalyst **8** is a C$_2$ symmetric molecule, the four hydrogens at the two alpha positions of the carbonyl moiety in complex pre-**iv** exist as two sets of diastereotopic hydrogens. For each couple, due to the steric hindrance of the base and to the poor overlap between equatorial C-H bond and C=O π* orbital, only the highlighted axial H$_a$ and H$_b$ protons are accessible (Scheme 5) and the energy associated to the deprotonation is 10.68 kcal mol^{-1} in one case and 9.15 kcal mol^{-1} in the other one. After the deprotonation step, cationic species **v** is formed by the expulsion of a chloride anion from hypervalent species **iv** and the transition state associated to this expulsion requires 26.22 kcal mol^{-1}. The four geometries of relative genuine TSs responsible of the *syn*- and *anti*- products formation were located using B3LYP-D3 functional with 6-31G(d,p) basis set (each with one negative imaginary frequency), then finer electronic energies of the optimized structure were successively obtained increasing the basis set up to 6-311+G(2df,2pd). The calculations, performed using (*S*)-TetraMe-BITIOPO **8** as catalyst, showed that transition states TS(**8**)-(**vi**)-**a**, and TS(**8**)-(**vi**)-**b,** responsible of the formation of the two *anti* diastereoisomers, are more stable in energy compared to transition states related to the formation of *syn* diastereoisomers. As shown, TS(**8**)-(**vi**)-**a**, responsible of the attack of the silylenol ether onto the *Re* face of the aldehyde, leads to the experimentally observed *anti*-(2*S*,1'*R*)-diastereoisomer,[16] and it is more stable by 0.47 kcal mol^{-1} than TS(**8**)-(**vi**)-**b**. A possible explanation of this slight difference between TS(**8**)-(**vi**)-**a** and TS(**8**)-(**vi**)-**b** could be ascribed to the presence of a steric repulsion between the diphenyl phosphinoyl group of (*S*)-TetraMe-BITIOPO phosphinoxide and the silylenol ether in TS(**8**)-(**vi**)-**b** (Figure 2).

Finally, the construction of the new carbon-carbon bond generates species *anti*-(**vii**) and *syn*-(**vii**) which release the Lewis base in the presence of *i*Pr$_2$NEt. In this way, the so generated trichlorosilyl compound **9** will then be converted into final product **6** after an aqueous work up. To validate our proposed model of stereoselection, we calculated also transition states TS(**7**)-(**vi**)-**a** and TS(**7**)-(**vi**)-**b**, where catalyst **8** has been replaced by (S)-BINAPO.

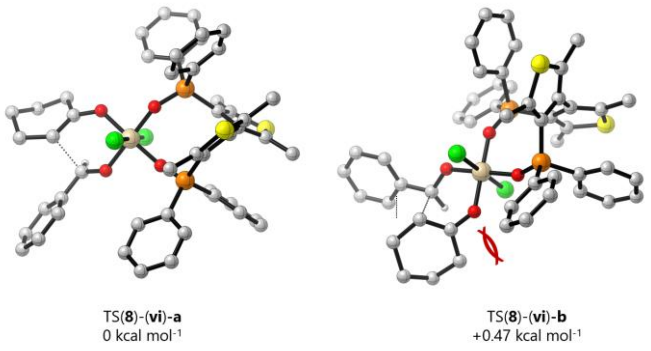

Figure 2: Geometries of TSs-(**8**)-(**vi**) responsible of the two (*anti*)-**6** isomers formation calculated at B3LYP-D3/6-311+G(2df,2pd) // B3LYP-D3/6-31G(d,p) level of theory.

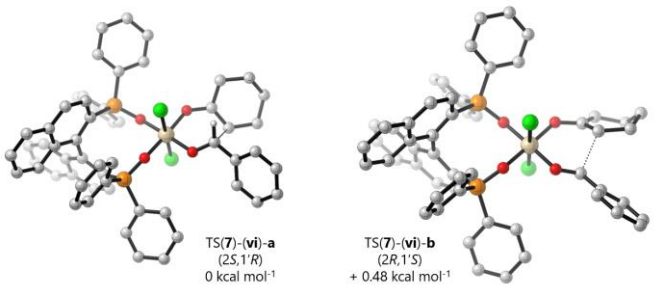

Figure 3: Geometries and $\Delta\Delta E^{\neq}$ of transitions states TSs-(**7**)-(**vi**) responsible of the two (*anti*)-**6** isomers formation, calculated at B3LYP-D3/6-311+G(2df,2pd) // B3LYP-D3/6-31G(d,p) level of theory.

As shown in the literature, (*S*)-BINAPO leads to the formation of β-hydroxy ketone (2*S*,1'*R*)-*anti*-**6**.[33] Gratefully, DFT calculations confirmed this trend, and TS(**7**)-(**vi**)-**a**, responsible of the formation of (2*S*,1'*R*)-*anti*-**6** product was found to be more favored of 0.48 kcal mol^{-1} than TS(**7**)-(**vi**)-**b** (Figure 3).

Unfortunately, the TS energy differences obtained for catalysts **7** and **8** are very similar, and although they are able to explain the sense of stereoselection, they are not sufficient to explain the improved stereochemical efficiency observed for (*S*)-TetraMe-BITIOPO (Scheme 3).

Since phosphineoxides can catalyze the cross aldol reaction between aromatic and an aliphatic aldehydes,[33] we decided to extend our computational analysis to the formation of 1-phenyl, 2,2-dimethyl propan-1,3-diol **10** by computational approach.

It is known that catalyst **8** is able to perform the cross condensation between benzaldehyde and isobutyraldehyde in CH_2Cl_2 as solvent in the presence of 3 equivalents of $SiCl_4$, followed by reduction of $NaBH_4$ (Scheme 7).[35] Under these reaction conditions, compound **10** can be isolated in modest yield and 70% ee for the (*S*)-enantiomer. Calculations at B3LYP-D3/6-311+G(2df,2pd) // B3LYP-D3/6-31G(d,p) level of theory revealed that TS-(**8**)-*Si,* accounting for the formation of the experimentally observed (*S*) enantiomer, is favored by 4.69 kcal mol^{-1} compared to TS-(**8**)-*Re*. Once again, this difference in energy can be ascribed to the presence of steric repulsions between the diphenyl phosphinoyl group and the aromatic ring of benzaldehyde in the disfavored transition state.

Conclusions

In conclusion, the mechanism of the direct, organocatalytic aldol reactions catalysed by a chiral cationic hypervalent silicon species, generated by coordination of tetraMe-BITIOPO to $SiCl_4$, has been investigated by DFT approach. The same approach was also extended to the stereoselective organocatalytic addition of silyl enol ethers to aromatic aldehydes catalysed by Denmark bisphosphoroamide.

These computational analysis confirm the previous empirical model proposed for these transformations and can offer useful suggestions for the design of new asymmetric catalysts as well as in the comprehension of other chemical transformations catalysed by phosphine oxides and mediated by $SiCl_4$.

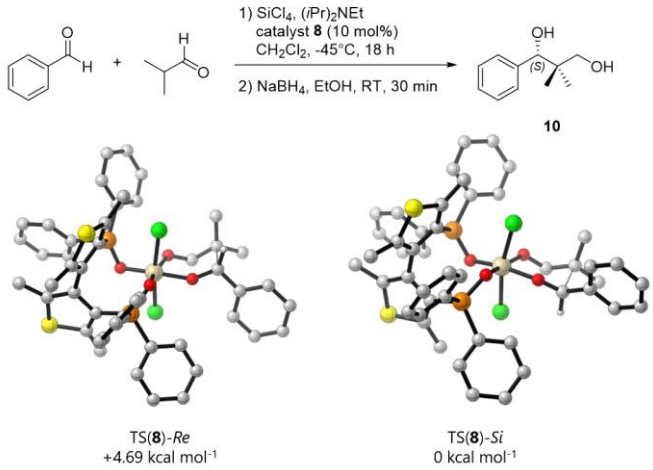

Scheme 7: Geometries and $\Delta\Delta E^{\neq}$ of transitions states related to cross aldol reaction between benzaldehyde and isobutyraldehyde calculated at B3LYP-D3/6-311+G(2df,2pd) // B3LYP-D3/6-31G(d,p) level of theory. *Re/Si* faces are defined considering the aromatic aldehyde.

Conflicts of interest

There are no conflicts to declare.

Acknowledgements

SR thanks Università degli Studi di Milano for PSR 2019 - financed project "Catalytic strategies for the synthesis of high added-value molecules from bio-based starting material" and CINECA (ISCRA_C project IsC74_Hy-SiPOs) for HPC facilities.

Notes and references

1 Gay-Lussac J.L. and T. J.A., *Mem. Phys. Chem. Soc. Arcueil*, **1809**, *2*, 317-331.
2 S. E. Denmark and G. L. Beutner, *Angew. Chem. Int. Ed.*, **2008**, *47*, 1560-1638.
3 M. Oestreich and S. Rendler, *Synthesis*, **2005**, 1727-1747.
4 Y. Orito and M. Nakajima, *Synthesis*, **2006**, 1391-1401.
5 S. Rossi and S. E. Denmark, in Lewis Base Catalysis in Organic Synthesis, John Wiley & Sons, Inc., **2016**, DOI: 10.1002/9783527675142.ch21, pp. 1039-1076.
6 M. Benaglia, S. Guizzetti and S. Rossi, in Catalytic Methods in Asymmetric Synthesis, John Wiley & Sons, Inc., **2011**, DOI: 10.1002/9781118087992.ch14, pp. 579-624.
7 S. Rossi and S. E. Denmark, in Organosilicon Chemistry, ed. M. O. Tamejiro Hiyama, Wiley-VCH, 1st. edn., **2019**, DOI: 10.1002/9783527814787.ch10, pp. 333-415.
8 O. J. Curnow, *J. Chem. Educ*., **1998**, 75, 910.
9 R. J. P. Corriu, J. C. Young, D. A. Armitage, R. J. P. Corriu, T. C. Kendrick, B. Parbhoo, T. D. Tilley, J. W. White and J. C. Young, in The Silicon–Heteroatom Bond (1991), John Wiley & Sons, Inc., **2010**, DOI: 10.1002/9780470772447.ch1, pp. 1-48.
10 S. Tandura, M. Voronkov and N. Alekseev, in Structural Chemistry of Boron and Silicon, Springer Berlin Heidelberg, **1986**, vol. 131, ch. 3, pp. 99-189.
11 J. I. Musher, *Angew. Chem. Int. Ed.*, **1969**, 8, 54-68.
12 12. W. B. Jensen, *Chem. Rev*., **1978**, 78, 1-22.

13 S. N. Tandura, M. G. Voronkov and N. V. Alekseev, **1986**, *131*, 99-189.
14 R. Gillespie, *Coord. Chem. Rev*., **2002**, 233-234, 53-62.
15 C. F. Matta and R. J. Gillespie, *J. Chem. Educ*., **2002**, 79, 1141.
16 G. Frenking, *Angew Chem Int Ed*, **2003**, *42*, 143-147.
17 R. F. W. Bader, *Monatshefte für Chemie - Chemical Monthly*, **2005**, *136*, 819-854.
18 W. B. Jensen, *J. Chem. Educ.,* **2006**, *83*, 1751.
19 J. Wagler, U. Böhme and E. Kroke, Higher-Coordinated Molecular Silicon Compounds, Springer International Publishing, **2013**.
20 V. Gutmann, *Coord. Chem. Rev*., **1975**, *15*, 207-237.
21 S. Rossi, M. Benaglia and A. Genoni, *Tetrahedron*, **2014**, 70, 2065-2080.
22 S. E. Denmark and J. R. Heemstra, Jr., *Org. Lett*., **2003**, *5*, 2303-2306.
23 S. E. Denmark, G. L. Beutner, T. Wynn and M. D. Eastgate, *J. Am. Chem. Soc.,* **2005**, *127*, 3774-3789.
24 G. A. Kaminski, R. A. Friesner, J. Tirado-Rives and W. L. Jorgensen, *J. Phys. Chem B*, **2001**, *105*, 6474-6487.
25 MacroModel, version 9.7, Schrodinger, LLC, New York, NY, **2009**
26 Small-Molecule Drug Discovery Suite 2016-4, Schrodinger, LLC, New York, NY, **2016**
27 Gaussian 16, Revision A.03, M. J. Frisch, G. W. Trucks, H. B. Schlegel, G. E. Scuseria, M. A. Robb, J. R. Cheeseman, G. Scalmani, V. Barone, G. A. Petersson, H. Nakatsuji, X. Li, M. Caricato, A. V. Marenich, J. Bloino, B. G. Janesko, R. Gomperts, B. Mennucci, H. P. Hratchian, J. V. Ortiz, A. F. Izmaylov, J. L. Sonnenberg, D. Williams-Young, F. Ding, F. Lipparini, F. Egidi, J. Goings, B. Peng, A. Petrone, T. Henderson, D. Ranasinghe, V. G. Zakrzewski, J. Gao, N. Rega, G. Zheng, W. Liang, M. Hada, M. Ehara, K. Toyota, R. Fukuda, J. Hasegawa, M. Ishida, T. Nakajima, Y. Honda, O. Kitao, H. Nakai, T. Vreven, K. Throssell, J. A. Montgomery, Jr., J. E. Peralta, F. Ogliaro, M. J. Bearpark, J. J. Heyd, E. N. Brothers, K. N. Kudin, V. N. Staroverov, T. A. Keith, R. Kobayashi, J. Normand, K. Raghavachari, A. P. Rendell, J. C. Burant, S. S. Iyengar, J. Tomasi, M. Cossi, J. M. Millam, M. Klene, C. Adamo, R. Cammi, J. W. Ochterski, R. L. Martin, K. Morokuma, O. Farkas, J. B. Foresman, and D. J. Fox, Gaussian, Inc., Wallingford CT, **2016**.
28 E. R. Johnson, S. Keinan, P. Mori-Sanchez, J. Contreras-Garcia, A. J. Cohen and W. Yang, *J. Am. Chem. Soc*., **2010**, *132*, 6498-6506.
29 J. Contreras-Garcia, E. R. Johnson, S. Keinan, R. Chaudret, J. P. Piquemal, D. N. Beratan and W. Yang, *J. Chem. Theory Comput*., **2011**, *7*, 625-632.
30 M. O. Sinnokrot, E. F. Valeev and C. D. Sherrill, *J. Am. Chem. Soc*., **2002**, *124*, 10887-10893.
31 M. Pitonak, P. Neogrady, J. Rezac, P. Jurecka, M. Urban and P. Hobza, *J. Chem. Theory Comput*., **2008**, *4*, 1829-1834.
32 S. E. Denmark and W. Lee, *Chem. Asian J*., **2008**, *3*, 327-341.
33 S. Kotani, Y. Shimoda, M. Sugiura and M. Nakajima, *Tetrahedron Lett*., **2009**, *50*, 4602-4605.
34 S. Rossi, M. Benaglia, F. Cozzi, A. Genoni and T. Benincori, *Adv. Synth. Catal.,* **2011**, *353*, 848-854.
35 S. Rossi, M. Benaglia, A. Genoni, T. Benincori and G. Celentano, *Tetrahedron*, **2011**, *67*, 158-166.
36 A. Genoni, M. Benaglia, S. Rossi and G. Celentano, *Chirality*, **2013**, *25*, 643-647.
37 S. Rossi, R. Annunziata, F. Cozzi and L. Raimondi, *Synthesis*, **2015**, *47*, 2113-2124.
38 S. Rossi, M. Benaglia, R. Cirilli and T. Benincori, *Asymmetric Catalysis*, **2015**, *2*, 17-25.
39 M. Abbinante, M. Benaglia, S. Rossi, T. Benincori, R. Cirilli, M. Pierini, *Org. Biomol. Chem*., **2019**, *17*, 7474-7481.
40 S. Rossi, T. Benincori, L. M. Raimondi, M. Benaglia, *Synlett*, **2020**, *31*, 535-546.
41 J. D. Short, S. Attenoux and D. J. Berrisford, *Tetrahedron Lett*., **1997**, **38**, 2351-2354.
42 S. E. Denmark, S. M. Pham, R. A. Stavenger, X. Su, K. T. Wong, Y. Nishigaichi, *J. Org. Chem*., **2006**, *71*, 3904-3922.
43 S. E. Denmark, B. M. Eklov, P. J. Yao and M. D. Eastgate, *J. Am. Chem. Soc.,* **2009**, *131*, 11770-11787.
44 S. E. Denmark, B. J. Williams, B. M. Eklov, S. M. Pham and G. L. Beutner, *J. Org. Chem.,* **2010**, *75*, 5558-5572.
45 S. Grimme, Wiley Interdisciplinary Reviews: Computational Molecular Science, **2011**, *1*, 211-228.
46 J. P. Wagner and P. R. Schreiner, *Angew. Chem. Int. Ed.*, **2015**, *54*, 12274-12296.
47 S. Grimme, J. Antony, S. Ehrlich, H. Krieg, *J. Chem. Phys*., **2010**, *132*, 154104.
48 S. E. Denmark and G. L. Beutner, in Lewis Base Catalysis in Organic Synthesis, ed. I. John Wiley & Sons, **2016**, DOI: 10.1002/9783527675142.ch2, pp. 31-54.

